Journal Name

COMMUNICATION

Charge-dependent hierarchical self-assembling of fluorinated gold nanoclusters.

Received 00th January 20xx,

Accepted 00th January 20xx

DOI: 10.1039/x0xx00000x

www.rsc.org/

Yuki Saito,[a] Duhong Sun,[b] Hayato Kanai, [c] Yasuhiro Ishida,[c] Hideyuki Mitomo,[d] Kuniharu Ijiro,[d] Katsuaki Konishi * [a,b]

$Au_{25}(SR)_{18}$ nanoclusters decorated with semifluorinated thiolate ligands (SFLs) self-assemble hierarchically depending on the charge state of the nanocluster component; the use of the anionic cluster ($[Au_{25}]^-$) resulted in the generation of nanofibers, whereas the neutral counterpart ($[Au_{25}]^0$) gave micron-sized filaments as a result of the bundling/twisting of the nanofibers.

The self-assembly of ligand-protected metal nanoclusters has recently attracted increasing interest because it can endow smart nanomaterials with unique structure-/morphology-dependent synergistic functions.[1-9] The simplest strategy to construct such cluster-based self-assemblies is to utilize interligand interactions coupled with control of the assembly conditions. Successful examples involving the use of directional attractive interactions such as hydrogen bonding have been reported.[1-3] On one hand, some ligand-protected nanoclusters are characterized by redox activity to have different oxidation states on the cluster core.[10-14] Therefore, in addition to the interligand attractive forces, electrostatic interactions could be used for the control of the morphology and nanostructures. However, such examples have not been reported.

In this paper, we report the unprecedented hierarchical self-assembly of gold clusters by combining attractive interactions and electrostatic repulsive forces. The main attractive force is fluorophilic interactions. Fluorine has the highest electronegativity among the elements that cause low dispersion forces in the perfluorinated units, which leads to the emergence of strong attractive forces between the perfluorinated moieties to facilitate controlled supramolecular assembling.[15, 16] The unique structure-directing capability of the fluorophilic interaction has been shown in the assembly of gold nanoparticles (d = ~10 nm) coated with multiple semifluorinated thiolate ligands (SFLs), which spontaneously assemble to give hollowed vesicles under particular conditions.[17, 18] Ligand-protected metal nanoclusters with much smaller sizes (d < ~2 nm) have recently emerged as smaller varieties of nanoparticles, but they essentially behave as molecules to display many different properties from conventional nanoparticles.[19, 20] In this respect, investigating the morphological features of nanoassemblies constructed from such miniatures is interesting. Here, we employed a Au_{25} cluster stabilized by 18 thiolate ligands (SR), which can take several charge states.[10-12] We demonstrate that the SFL-modified $[Au_{25}]^-$ cluster spontaneously assembles into nanofibers with a diameter of 30–50 nm upon simple evaporation from a solution. Notably, when the starting cluster was oxidized into the electrically neutral form($[Au_{25}]^0$), the nanofibers further assembled to give twisted bundles with a μm-order diameter. This work demonstrates an example of the control of the nanoscale and mesoscale structural hierarchy of cluster-based nanoassemblies through the combination of the fluorophilic interactions of ligand moieties and the electrostatic interactions of gold cores.

The precursor thiol for SFL modification (**Fig. 1a**) was synthesized and introduced to the surface of the Au_{25} cluster via the ligand exchange reaction by following the synthetic methods of the SFL-modified nanoparticles.[13] Typically, $[Au_{25}(HT)_{18}](TOA)$ (HT = 1-hexanethiolate, TOA = tetraoctylammonium) was reacted with SFL-H (30 molar eq.) in THF for 5 h under ambient conditions to yield the SFL-modified Au_{25} cluster $[Au_{25}(SFL)_x(HT)_{18-x}]^-$ (**1a**) after purification by size exclusion chromatography (SEC). The degree of SFL introduction was x = ~15 on average, as estimated from the ^{1}H NMR spectrum of the reaction mixture (**Fig. S1**). Immediately after SEC isolation, the solution of **1a** remained homogeneous in

[a] *Faculty of Environmental Earth Science, Hokkaido University, North 10 West 5, Sapporo 060-0810 (Japan).*
[b] *Graduate School of Environmental Science, Hokkaido University, North 10 West 5, Sapporo 060-0810 (Japan).*
[c] *RIKEN Center for Emergent Matter Science2-1 Hirosawa, Wako, Saitama 351-0198 (Japan).*
[c] *Research Institute for Electronic Science, Hokkaido University, North 21 West 10, Sapporo 001-0021 (Japan).*
† Footnotes relating to the title and/or authors should appear here.
Electronic Supplementary Information (ESI) available: [details of any supplementary information available should be included here]. See DOI: 10.1039/x0xx00000x

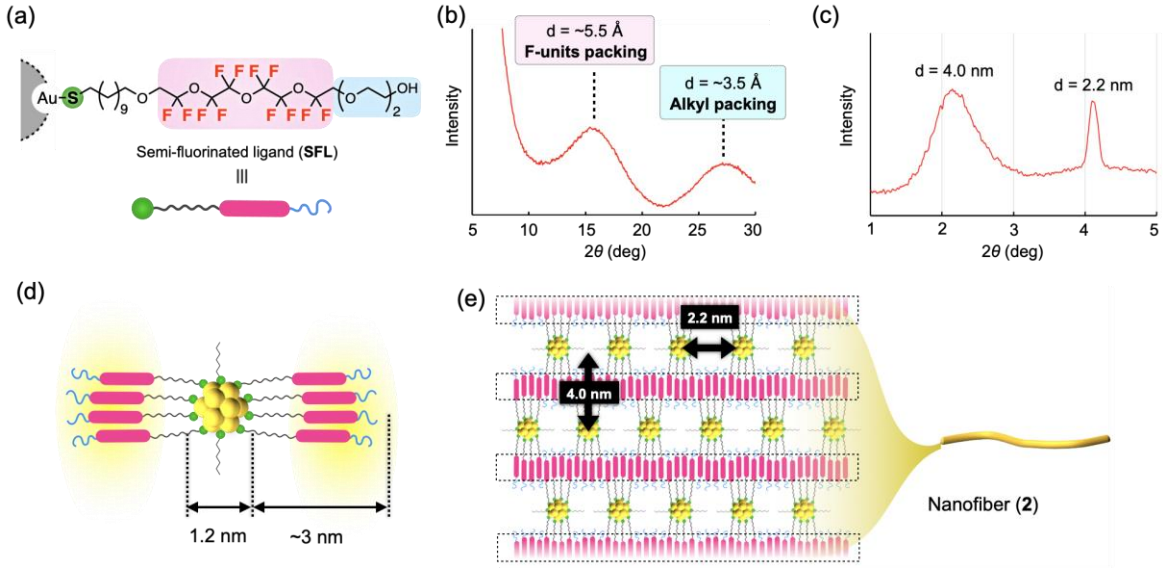

Fig. 1. (a) Structure of semifluorinated ligand deposited on gold cluster surface. (b) PXRD and (c) SAXS patterns of the nanofiber **2**. (d) Anisotropic ligand orientation of the SFL-modified Au_{25} cluster. (e) A possible arrangement of the gold clusters in nanofiber **2** deduced based on the SAXS profiles.

THF, and the DLS profile revealed no signs of extended aggregation (**Fig. S2**). However, upon evaporation with a conventional rotary evaporator, fibrous nano-objects with diameters of several tens of nanometers were found in the scanning electron microscopy (SEM) images (**Fig. 2a-d**). The transmission electron microscopy (TEM) (**Fig. 2e**) revealed that the nanofibers are composed of ultrasmall gold clusters, which excludes the possibility of the fusion of the clusters. The expanded image at the end of a nanofiber showed a circular cross-section (**Fig. 2d**), showing that the fibers have cylindrical structures.

The formation of nm-order fibers (**2**) from the molecular-sized cluster (**1a**) is considered driven by the interligand fluorophilic interaction. To confirm this point, a nonfluorinated analogue, in which fluorine atoms are substituted with hydrogen atoms, was synthesized similarly. As shown in the SEM image (**Fig. 2f**), no characteristic structural features were observed, indicating the critical role of the SFL ligands in the formation of nanofibers. The nanostructure of **2** was further investigated by X-ray diffraction. The scattering patterns of powder X-ray diffraction (PXRD) analysis of **2** showed two broad peaks at 2θ = 16° and 27°, which correspond to *d* spacings of ~0.55 and ~0.35 nm, respectively (**Fig. 1b**). On the basis of the reported diffraction patterns,[21,22] the longer one is assignable to the packed fluorinated units whereas the shorter one to the alkyl chains. Thus, considering the difference in the nature of the attractive forces, each of them would assemble in a self-sorting manner to give phase-segregated domains.

We next investigated the mesoscale ordering of the Au clusters in the nanofiber (**2**) by using small angle X-ray scattering (SAXS). As shown in **Fig. 1c,** two distinct peaks were observed at 2θ = 2.3 and 4.1°, indicating the presence of lattice planes with *d* spacings of 4.0 and 2.2 nm, respectively. This result implies that the Au clusters in the nanofiber are not randomly aggregated but rather take a particular arrangement. Considering the bulkiness of TOA^+, counterions seem not to be included in the nanofiber, rather residing outside. On one hand, the Å-level periodicity of the fluorinated segments, which was shown in the PXRD profile (**Fig. 1b**), suggests that SFLs are anisotropically oriented on the cluster surface to allow the formation of several sets of aligned SFL units (**Fig. 1d**). This may allow long-range self-assembly of the SFL units through fluorophilic interactions. The anisotropic ligand orientation

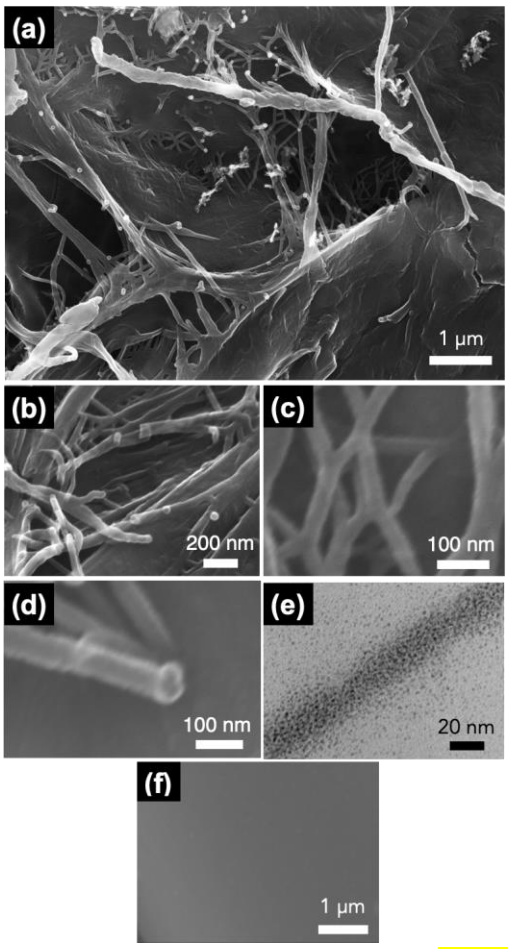

Fig. 2. SEM (a-d) and TEM (e) images of the nanofiber **2.** (f) SEM image of the corresponding non-fluorinated cluster.

seems unusual because it would be entropically unfavorable. However, such behaviors have been reported in the vesicles of SFL-modified Au nanoparticles[17] and in the 2D sheet of the MBA (4-mercaptobenzoic acid)-protected Au_{102} cluster.[1-3]

On the basis of the above structural information, a possible arrangement in the nanofiber (**2**) is schematically depicted in **Fig. 1e**. Considering the size of the extended SFL unit (~ 3.0 nm), the lattice-plane distance of ~4.0 nm (2θ = 2.3°), which was shown in the SAXS profile (**Fig. 1c**), indicates that the cluster columns are separated by the interdigitated SFL blocks that are clipped by the fluorinated segments assembled through fluorophilic interactions (shown in the dotted boxes in **Fig. 1e**). Accordingly, the fluorinated moieties of SFL serve as glues to bridge the cluster columns. This arrangement can give rise to additional diffractions, which are in accordance with the peak observed at 2θ = 4.1° (d = 2.2 nm). Taken together, the self-assembly of **1a** appears to be governed by the attractive interactions of the SFL units. Although other attractive interactions, such as van der Waals forces of glycol and alkyl units, can be involved, the fluorophilic interaction appears to be primarily important because the solvophobic effects owing to the fluorinated moieties would become pronounced during the evaporation process. The self-assembly direction of the fluorinated units may be associated with the anisotropic morphology of **2**. Thus, the growth reaction may proceed preferentially in accordance with the development of arrays of fluorinated units, thereby affording nanofibers with crystalline segments.

For the above Au cluster-based nanofiber (**2**), we utilized anionic **1a** as the starting material. Therefore, the nanofibers are ionic and should accompany counter cations (TOA^+), which may affect the self-assembly processes. To obtain insights, we investigated the morphology of the assembly derived from the neutral derivative of **1a** ($[Au_{25}]^0$, **1b**). **1b** was prepared by a similar ligand exchange reaction of neutral $[Au_{25}(HT)_{18}]$, which was obtained via silica gel-mediated oxidation according to the literature.[11] The SEM image of the solid samples of **1b** (**3**) obtained by evaporation of the THF solution also exhibited fibrous features, but the size scale and overall morphology were rather different (**Fig. 3a, b**). Curled filaments with a μm-order thickness were observed, which are more sizable than the nanofibers (**2**) prepared from anionic **1a**. Interestingly, the TEM image (**Fig. 3c**) revealed that the ribbon architectures are composed of string-like nanofibers. The diameters of the strings were approximately 30 nm, which are comparable to the sizes of the nanofibers of **2** (**Fig. 2**). Therefore, the μm-order filaments (**3**) might have formed as a result of the bundling of nanofibers. Namely, self-assembly of the neutral Au_{25} cluster (**1b**) is considered to occur hierarchically. Notably, bundled nanofibers were sometimes further twisted to form helical or double-helix structures (**Fig. 3a, b**), showing a unique example of helical self-assembled structures of achiral nanoclusters.[23, 24]

The notable differences in the hierarchical features and size scales between assemblies **2** and **3**, which were derived from anionic $[Au_{25}]^-$ (**1a**) and neutral $[Au_{25}]^0$ (**1b**), respectively, suggest that electrostatic interactions play a key role in determining the course of self-assembly. Considering the similarity in the sizes and morphological features of the minimal fibrous objects found in **2** and **3** (**Figs. 2** and **3a**), the first self-assembly events seem to be dominated by the fluorophilicity of the SFL units, which leads to the anisotropic arrangement of the cluster molecules. The surfaces of the first-generation fibrous assemblies from the neutral $[Au_{25}]^0$ cluster (**1b**) may readily adhere to each other through van der Waals forces to give bundled nanofibers (**Fig. 3d**). On the other hand, with anionic **1a**, such weak attractive interactions are

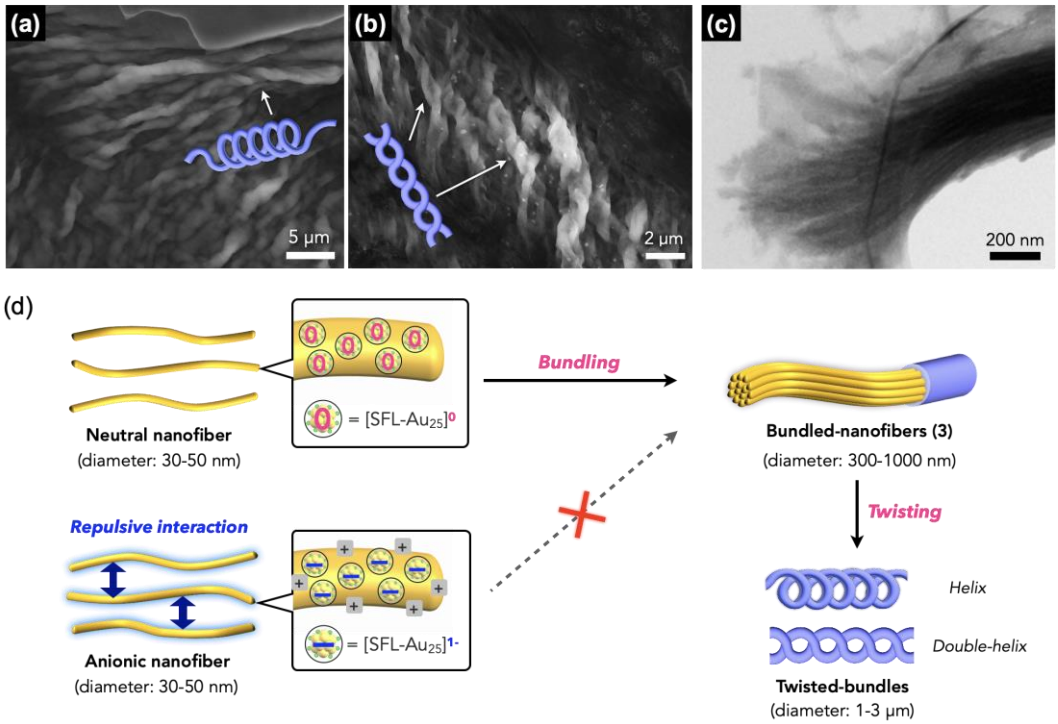

Fig. 3. (a, b) SEM and (c) TEM images of **3** derived from neutral $[Au_{25}]^0$ clusters. (d) Schematic illustration of the hierarchy of the assembling of SFL-modified Au_{25} clusters. The bundling is unlikely to occur when the component Au_{25} cluster is anionic state due to the large repulsive interaction between nanofibers.

hampered presumably because of the electrostatic repulsion between the ionic nanofiber surfaces and steric hindrance of the accompanying bulky TOA^+. Thus, their original discrete forms are retained (**Fig. 2**). Although further structural studies as well as the elucidation of the structure-directing factors (e.g. counterions) are needed, the present results imply that the hierarchical assembly modes can be changed by tuning the ionic characteristics of the molecular components.

The above fibrous cluster solids (**2** and **3**) were soluble in the original solvent (THF), suggesting that they are essentially constructed from small components via noncovalent forces. Accordingly, the absorption spectra of the homogeneous solutions obtained from the solid samples (**2** and **3**) gave characteristic patterns of $[Au_{25}]^-$ and $[Au_{25}]^0$, respectively (**Fig. S3**), indicating that the original Au_{25} frameworks and charge states were essentially retained during the assembly/disassembly processes. However, the DLS profiles of the redissolved solutions revealed hydrodynamic diameters of approximately 50 nm (**Fig. S4**), which are definitely larger than those of the starting monomeric cluster (**1**). Therefore, the nanofibers found in the microscopy images were converted into small cluster aggregates rather than dispersed monomers. Owing to the solvophobic nature of fluorinated segments, once-formed fluorophilic interactions cannot be collapsed completely by solvent treatment (THF), resulting in small aggregates. These results are consistent with the critical involvement of the fluorophilic interaction in the self-assembly of the SFL-modified clusters.

In conclusion, we have shown the self-assembling behavior of Au_{25} clusters protected by semifluorinated thiolate ligands. Discrete nanofibers were obtained from $[Au_{25}]^-$, which may result from the fluorophilicity-mediated formation of ordered arrays of fluorinated units. On the one hand, with the neutral counterpart ($[Au_{25}]^0$), the nanofibers were further bundled to give μm-order filaments, thus showing an example of hierarchical assembly dependent on the charge state of the cluster component. The Au_{25} monomer we used here is structurally symmetrical, carrying multiple ligands that are spread isotropically from the inorganic core. In this respect, the role of the fluorinated segments in the self-assembly process is noteworthy. The strong intermolecular/intramolecular fluorophilic interactions likely break the structural symmetry of the cluster to allow anisotropic self-assembling in accordance with the growth of ordered fluorinated arrays. This work highlights the usefulness of shell and core-state engineering for the creation of hierarchical self-assembled structures of zero-dimensional nanoscale components.

This research was partly supported by the Photo-excitonix Project in Hokkaido University, MEXT/JSPS Grants-in-Aid to KK (KAKENHI 21H0468301). We also thank Mr. T. Tanioka for help in TEM measurements.

Conflicts of interest

There are no conflicts to declare.

Notes and references

1. Y. Saito, C. Murata, M. Sugiuchi, Y. Shichibu and K. Konishi, *Coord. Chem. Rev.*, 2022, **470**, 214713.
2. Z. Wu, Q. Yao, S. Zang and J. Xie, *ACS Mater. Lett.*, 2019, **1**, 237-248.
3. Nonappa and O. Ikkala, *Adv. Funct. Mater.*, 2017, **28**, 1704328.
4. Z. Wu, J. Liu, Y. Gao, H. Liu, T. Li, H. Zou, Z. Wang, K. Zhang, Y. Wang, H. Zhang and B. Yang, *J. Am. Chem. Soc.*, 2015, **137**, 12906-12913.
5. M. Sugiuchi, J. Maeba, N. Okubo, M. Iwamura, K. Nozaki and K. Konishi, *J. Am. Chem. Soc.*, 2017, **139**, 17731-17734.
6. Z. Wu, Y. Du, J. Liu, Q. Yao, T. Chen, Y. Cao, H. Zhang and J. Xie, *Angew. Chem., Int. Ed.*, 2019, **58**, 8139-8144.
7. M. Sugiuchi, M. Zhang, Y. Hakoishi, Y. Shichibu, N. N. Horimoto, Y. Yamauchi, Y. Ishida and K. Konishi, *J. Phys. Chem. C*, 2020, **124**, 16209-16215.
8. Q. Yao, L. Liu, S. Malola, M. Ge, H. Xu, Z. Wu, T. Chen, Y. Cao, M. F. Matus, A. Pihlajamaki, Y. Han, H. Hakkinen and J. Xie, *Nat. Chem.*, 2023, **15**, 230-239.
9. Y. Saito, A. Suda, M. Sakai, S. Nakajima, Y. Shichibu, H. Kanai, Y. Ishida and K. Konishi, *Chem. Sci.*, 2024, **15**, 11775-11782.
10. M. Zhu, W. T. Eckenhoff, T. Pintauer and R. Jin, *J. Phys. Chem. C*, 2008, **112**, 14221-14224.
11. S. Antonello, G. Arrigoni, T. Dainese, M. De Nardi, G. Parisio, L. Perotti, A. Rene, A. Venzo and F. Maran, *ACS Nano*, 2014, **8**, 2788-2795.
12. D. R. Kauffman, D. Alfonso, C. Matranga, P. Ohodnicki, X. Deng, R. C. Siva, C. Zeng and R. Jin, *Chem. Sci.*, 2014, **5**.
13. Y. Kamei, Y. Shichibu and K. Konishi, *Angew. Chem., Int. Ed.*, 2011, **50**, 7442-7445.
14. Y. Kamei, N. Robertson, Y. Shichibu and K. Konishi, *J. Phys. Chem. C*, 2015, **119**, 10995-10999.
15. J. Calvo-Castro, G. Morris, A. R. Kennedy and C. J. McHugh, *Crystal Growth & Design*, 2016, **16**, 5385-5393.
16. Z. M. Hudson, J. Qian, C. E. Boott, M. A. Winnik and I. Manners, *ACS Macro Letters*, 2015, **4**, 187-191.
17. K. Niikura, N. Iyo, T. Higuchi, T. Nishio, H. Jinnai, N. Fujitani and K. Ijiro, *J. Am. Chem. Soc.*, 2012, **134**, 7632-7635.
18. J. Wei, K. Niikura, T. Higuchi, T. Kimura, H. Mitomo, H. Jinnai, Y. Joti, Y. Bessho, Y. Nishino, Y. Matsuo and K. Ijiro, *J. Am. Chem. Soc.*, 2016, **138**, 3274-3277.
19. R. Jin, C. Zeng, M. Zhou and Y. Chen, *Chem. Rev.*, 2016, **116**, 10346-10413.
20. I. Chakraborty and T. Pradeep, *Chem. Rev.*, 2017, **117**, 8208-8271.
21. E. L. Heeley, D. J. Hughes, Y. El Aziz, P. G. Taylor and A. R. Bassindale, *Macromolecules*, 2013, **46**, 4944-4954.
22. L. Sosa-Vargas, F. Nekelson, D. Okuda, M. Takahashi, Y. Matsuda, Q.-D. Dao, Y. Hiroyuki, A. Fujii, M. Ozaki and Y. Shimizu, *J. Mater. Chem. C*, 2015, **3**, 1757-1765.
23. J. Liu, Y. Tian, L. Ai, Z. Wu, D. Yao, Y. Liu, B. Yang and H. Zhang, *Langmuir*, 2020, **36**, 14614-14622.
24. M. Lipok, P. Obstarczyk, S. Parzyszek, Y. Wang, M. Bagiński, T. Buergi, W. Lewandowski and J. Olesiak − Bańska, *Adv. Opt. Mater.*, 2022, **11**, 2201984.

